regions of galaxies[19]. At this moment, it is not obvious how the gas disks will respond to pressure due to the Magnus effect. The hydrodynamical simulations become essential to understand the effect on star formation and galaxy morphology.

A possible instance of the Magnus effect can be attributed to widespread observation of gas lopsidedness in galaxies. It has been known that gaseous and stellar mass distribution in disk galaxies may not be strictly axisymmetric[20]. It now appears that non-axisymmetry or lopsidedness in disk galaxies is a general phenomenon[21]. The strength of lopsidedness is generally higher at larger radii in disks. The origin of lopsidedness is not yet well-understood. A recent review on this subject can be found in the literature[21]. The main problem in various theories proposed to explain lopsidedness lies in sustaining any non-axisymmetry over a few Galactic rotations, which will tend to dilute any kind of non-axisymmetry. Since a large fraction of galaxies show lopsidedness, the mechanism must be acting globally and all the time. The Magnus effect is such a mechanism which can act everywhere and all times in typical galactic environments.

We speculate that the Magnus effect is playing some role in maintaining various gaseous morphological asymmetries in galaxies. It may also be playing a role in modifying star formation rate in the outer regions of the disk, thereby introducing stellar lopsidedness as well. It is to be noted that at high redshifts, the IGM density scales up by $(1 + z)^3$ and therefore outcomes due to the Magnus effect may be crucial at the epochs of formation of galaxies in the past. The hydrodynamical simulations are currently planned to examine the Magnus effect in disk galaxies in different environments.

1. Magnus, G., Über die Abweichung der Geschosse, und: Über eine abfallende Erscheinung bei rotirenden Körpern. *Ann. Phys.*, 1853, **164**, 1–29.
2. Kundu, P. K. and Cohen, I. M., *Fluid Mechanics*, Academic Press, 2008.
3. Batchelor, G. K., *An Introduction to Fluid Dynamics*, Cambridge University Press, 1967.
4. Kahn, F. D. and Woltjer, L., Intergalactic matter and the galaxy. *Astrophys. J.*, 1959, **130**, 705–717.
5. Gunn, J. E. and Gott, J. R., On the infall of matter into clusters of galaxies and some effects on their evolution. *Astrophys. J.*, 1972, **176**, 1–20.
6. Livio, M. M., Regev, O. and Shaviv, G., On the role of viscosity in clusters of galaxies. *Astron. Astrophys.*, 1978, **70**, L7–L9.
7. Nulsen, P. E. J., Transport processes and the stripping of cluster galaxies. *Mon. Notes R. Astron. Soc.*, 1982, **198**, 1007–1016.
8. Ikeuchi, S. and Tomisaka, K., Interaction of intergalactic-gas-flow with a rigid-body-spheroidal galaxy. *Astrophys. Space Sci.*, 1981, **80**, 483–500.
9. Dyson *et al*. (eds), In *Diffuse Matter from Star Forming Regions to Active Galaxies*, Springer, 2006.
10. Schuecker, P., Finoguenov, A., Miniati, F., Bhringer, H. and Briel, U. G., Probing turbulence in the Coma galaxy cluster. *Astron. Astrophys.*, 2004, **426**, 387–397.
11. Woong-Tae, K., Heating and turbulence driving by galaxy motions in galaxy clusters. *Astrophys. J.*, 2007, **667**, L5–L8.
12. Perez-De-Tejada, H., Viscous magnus force for the rotating Venus ionosphere. *Astrophys. J.*, 2008, **676**, L65–L68.
13. Mulchaey, J. S., X-ray properties of groups of galaxies. *Annu. Rev. Astron. Astrophys.*, 2000, **38**, 289–335.
14. Honma, M. and Sofue, Y., On the Keplerian rotation curves of galaxies. *Publ. Astron. Soc. Jpn.*, 1997, **49**, 539–545.
15. Courteau, S. and Van Den Bergh, S., The solar motion relative to the local group. *Astron. J.*, 1999, **118**, 337–345.
16. Sembach, K. R. *et al*., Highly ionized high-velocity gas in the vicinity of the galaxy. *Astrophys. J. Suppl.*, 2003, **146**, 165–208.
17. Boulares, A. and Cox, D. P., Galactic hydrostatic equilibrium with magnetic tension and cosmic-ray diffusion. *Astrophys. J.*, 1990, **365**, 544–558.
18. Roediger, E. and Bruggen, M., Ram pressure stripping of disc galaxies: the role of the inclination angle. *Mon. Notes R. Astron. Soc.*, 2006, **369**, 567–580.
19. Kapferer *et al*., The effect of ram pressure on the star formation, mass distribution and morphology of galaxies. *Astron. Astrophys.*, 2009, **499**, 87–102.
20. Baldwin, J. E., Lynden-Bell, D. and Sancisi, R., Lopsided galaxies. *Mon. Not. R. Astron. Soc.*, 1980, **193**, 313–319.
21. Jog, C. J. and Combes, F., Lopsided spiral galaxies. *Phys. Rep.*, 2009, **471**, 75–111.

ACKNOWLEDGEMENTS. I acknowledge interesting and useful discussions with R. Nityananda and A. Manglam. I thank the referee for the comments which greatly improved the clarity of the contents in the paper.

Received 30 April 2010; revised accepted 21 February 2011

Development of cesium fountain frequency standard at the National Physical Laboratory, India

Amitava Sen Gupta, Ashish Agarwal, Poonam Arora* and Kavindra Pant

National Physical Laboratory (CSIR), Dr K. S. Krishnan Marg, New Delhi 110 012, India

We discuss the design and development of the cesium fountain frequency standard at the National Physical Laboratory, India. The optical set-up of the fountain needed to capture, cool, launch and detect the cesium atoms is discussed in detail. The concept and design of physical structure of the fountain is also described. In addition, some of our recent results on cooling and trapping of cesium atoms are reported.

Keywords: Atomic clocks, frequency control, laser cooling and trapping, magnetic shielding.

CESIUM (Cs) fountain frequency standards provide precise and accurate measurements of time and frequency.

*For correspondence. (e-mail: arorap@mail.nplindia.ernet.in)

Such atomic fountains are being developed at several laboratories around the world[1–12], and a few of them operate as primary frequency standards. At the National Physical Laboratory, India (NPLI), we started developing the country's first cesium fountain frequency standard a few years ago. The aim of this entire activity is to build a primary frequency standard for India with a relative uncertainty better than 1×10^{-15}.

The NPLI fountain has a (0, 0, 1) geometry of the magneto-optical trap (MOT) for cooling and launching operations. In this geometry, four out of the six cooling beams are in the horizontal plane and the others go up and down respectively. Whereas in the (1, 1, 1) geometry, where the beam orientation is such that there are three upward-travelling beams and three downward-travelling beams, all of which make an angle of $\pm 35.3°$ with the horizontal plane. The (0, 0, 1) is the most conventional, comparatively less sensitive to intensity imbalances, and is experimentally simple to handle. Furthermore, in order to launch the atoms in this geometry, only two beams are frequency detuned, whereas in (1, 1, 1) all six beams have to be frequency detuned for launch.

The atoms are first loaded and cooled in MOT followed by further cooling in optical molasses (OM). They are launched using moving molasses and cooled further with polarization gradient cooling. The design of various parts of the fountain such as optical system, physics package, electronics and microwave controls is discussed below.

The optical system delivers three mutually orthogonal pairs of counter-propagating laser beams, which are well balanced with respect to their intensities (5 mW/cm^2 each) and have diameters of about 15 mm each for the horizontal beams and 10 mm each for the vertical beams. There are two vertical beams – upward and downward (z-axis) and four horizontal beams, counter-propagating along the x-axis and the y-axis of a Cartesian coordinate system respectively. Besides the six cooling beams, the optical system delivers two beams for detection.

Our optical set-up provides the means for changing the laser intensity and frequency ν_c in a precisely controlled way in order to properly cool, launch and detect the atoms. Generation of cooling, re-pump, launch and detection beams, and finally coupling them into eight single-mode polarization maintaining (SM–PM) optical fibres is done on an environmentally controlled, vibration-free optical table of dimensions 1 m × 1.9 m. An extended cavity diode laser (ECDL) in Littrow configuration is frequency-locked to a Cs D_2 line (crossover peak of ^{133}Cs $6^2S_{1/2}$ ($F = 4$) → $6^2P_{3/2}$ ($F' = 4$ and 5) at 852 nm), generated by high resolution saturated absorption spectroscopy. Figure 1 shows the saturated absorption spectrum of Cs D2 line using ECDL.

The frequency and intensity of all the beams is controlled by acousto-optic modulators (AOMs) in a double pass configuration[13]. Figure 2 shows the diffraction efficiency as RF input frequency to AOM is changed. The measured single-pass bandwidth is found to be 34 MHz, whereas the double-pass bandwidth is 42 MHz. In addition, home-built fast mechanical shutters are used to eliminate residual scattering of resonant light during the Ramsey interrogation time. As shown in Figure 3, we use five AOMs to achieve the desired frequency and intensity control of cooling and detection beams. RF frequency of AOM1 is kept at 110 MHz, AOM2 frequency operates between 75 and 95 MHz, AOM3 frequency is fixed at 70 MHz, whereas AOM4 and AOM5 frequencies are 70 MHz for cooling and 70 ± $\delta\nu$ MHz for the launching.

RF input for AOM2 has the provision of fast frequency and amplitude sweep for the polarization gradient cooling process.

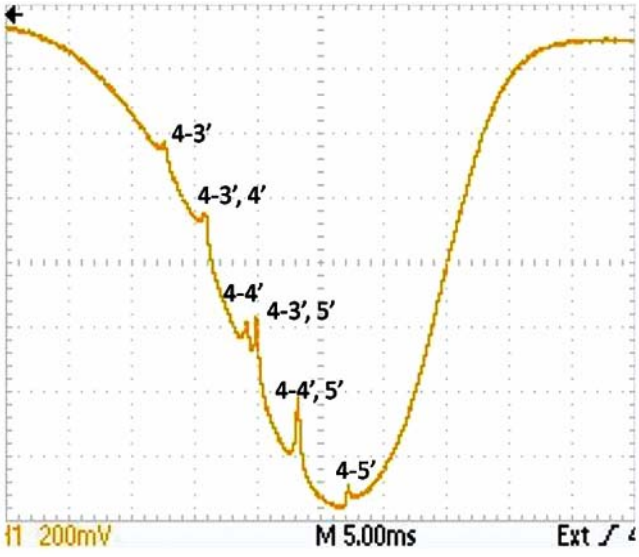

Figure 1. Saturated absorption spectrum of cesium D2 line with extended cavity diode laser.

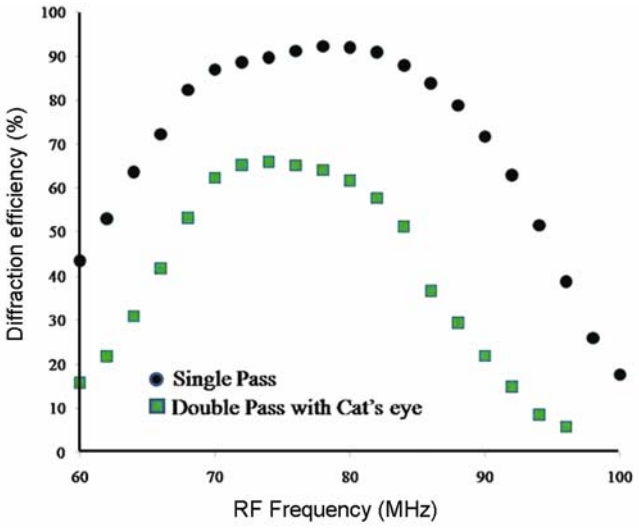

Figure 2. Measured diffraction efficiencies for acousto-optic modulators (AOMs) in single-pass and double-pass configurations.

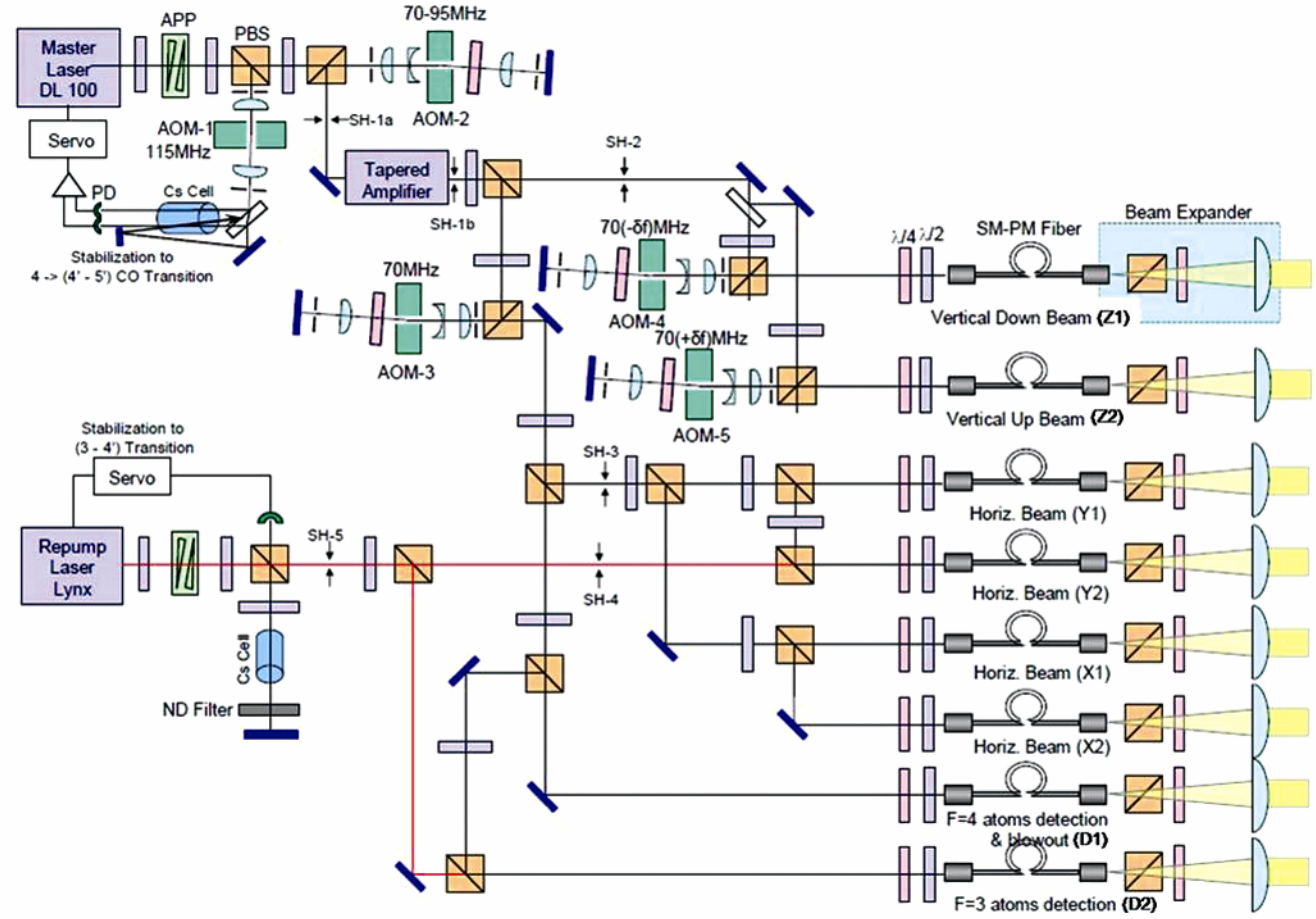

Figure 3. Schematic of optical system of the fountain at the National Physical Laboratory, India.

The double pass AOM2 output is used to seed the tapered amplifier TA-100 system which produces frequency-locked optical power of about 400 mW at the desired frequency. A combination of half wave plate and polarizing beam splitter (PBS) is used to split the TA output and direct it to each of the three cat's eye double-pass arrangements of AOM3, AOM4 and AOM5 for frequency and intensity control. The output of AOM3 is further split into six separate beams for cooling and detection. These are four horizontal cooling beams *X*1, *X*2, *Y*1 and *Y*2 and two detection beams *D*1 and *D*2 respectively. The AOM4 and AOM5 outputs produce the two vertical beams *Z*1 and *Z*2, which can be independently oppositely detuned for launching.

While the cooling laser beams address the cyclic transition $6^2S_{1/2}$ $F = 4 \rightarrow 6^2P_{3/2}$ $F' = 5$, non-resonant, spontaneous emission populates $6^2S_{1/2}$ $F = 3$ level eventually. To avoid such a population trapping in $6^2S_{1/2}$ $F = 3$ level, a second (re-pumping) laser is tuned and locked to the transition ^{133}Cs $6^2S_{1/2}$ $(F = 3,\ M_f = 0) \rightarrow 6^2P_{3/2}$ $(F' = 4,\ M_f = 0)$ also by saturated absorption spectroscopy. The locked re-pump beam is split and mixed with one of the cooling beams *Y*2 and the detection beam D_2.

The six cooling/re-pump beams and two detection beams are delivered from the optical table to the physics package using 10 m long SM–PM fibres. Coupling into the fibres is done using specially designed fibre couplers consisting of a miniature lens and a fibre holder. Fine adjustments of the lens focus and positions of the lens and the fibre tip are needed in order to optimize the transmission efficiency through the fibres which is around 55% for each of the eight fibres.

At the output end of the fibres, the beams are collimated with home-built beam expanders that produce the desired beam size and polarization. Our beam expander consists of a fibre holder with tip and tilt arrangement, a mount for holding the PBS, a quarter wave plate (QWP) and a movable 50 mm diameter achromatic plano-convex lens. The lens position is translated to get perfectly collimated Gaussian beams. QWP is suitably rotated to get the desired circular polarization for MOT beams.

The physics package of the fountain is shown in Figure 4. The structure has a base area of 0.85 m^2 and is 2 m tall and it is divided into four main levels. Level 1 contains the two 20 l/s ion pumps, level 2 contains the MOT and the fluorescence detection region, level 3 contains the

aluminium drift tube and magnetic shields, and level 4 has the two 55 l/s ion pumps and the optics for the vertically downward beam.

The Cs atoms are cooled in MOT followed by OM in an octagonal stainless steel chamber with five optical viewports on the sides and one at the bottom. The viewport at the top is provided in the vacuum enclosure in level 4. Two coils, each of 75 mm radius and 100 turns, in anti-Helmholtz configuration are used to create a magnetic field gradient of 6 G/cm at the centre of MOT. In addition, three pairs of rectangular Helmholtz coils (in *X*–*Y*–*Z* directions) around MOT region compensate the residual magnetic field at the centre of MOT. The source of Cs is a temperature-controlled cold finger attached to MOT chamber on the side. The temperature of the source is normally maintained at 10°C to generate adequate Cs vapour pressure in the chamber.

The fluorescence detection region lies between the fountain drift tube and MOT. The two horizontal, parallel detection beams, separated by 45 mm in vertical direction, are made of 10 mm square shape with the help of apertures. The corresponding fluorescence collector ensembles for the atoms in the two states $F = 4$ and $F = 3$ are placed in the direction perpendicular to the detection laser beams. Each ensemble consists of a pair of achromatic plano-convex imaging lenses (50 mm diameter and 75 mm focal length), placed back-to-back, to focus light onto a large-area silicon photodiode (10 mm square).

The entire vacuum hardware is made of stainless steel, except the drift tube which is made of aluminium. Individual vacuum subassemblies in the atom cooling and trapping zones (levels 1 and 2), drift zone (level 2) and top zone (level 3) have been initially individually assembled and tested for vacuum leaks. For vacuum joints between stainless steel and aluminium HELICOFLEX® gaskets are used. After the complete vacuum assembly of the fountain, we achieve a pressure of 6×10^{-10} torr without the Cs load.

The drift region is magnetically shielded using three layers of mu metal enclosures that result in an overall shielding factor of about 10^5. A uniform C-field is produced using a solenoid having 320 turns wound on a former with a diameter of 235 mm and length of 640 mm. The solenoid is placed inside the innermost magnetic shield and together with three additional compensation coils at the top and bottom, produces a homogeneous C-field of about 100 nT over the drift region. As shown in Figure 5, the initial measurements indicate the homogeneity of the C-field to be about 1 nT.

The Ramsey microwave interrogation of the atoms is proposed to be performed using a cylindrical cavity made of oxygen free high conductivity (OFHC) copper with a TE011 mode and quality factor of $Q_{\text{load}} \approx 2000$. This cavity is identical with that used in CsF1 of PTB, Germany and has been designed and fabricated there[12,14]. The Ramsey cavity is mounted inside the drift region and is 500 mm above the MOT centre. Another cavity made of OFHC copper is used for state selection and sits just below the Ramsey cavity. The source for the microwave interrogation is a synthesizer that has been designed in collaboration with PTB[15]. In this, a 9600 GHz YIG oscillator is

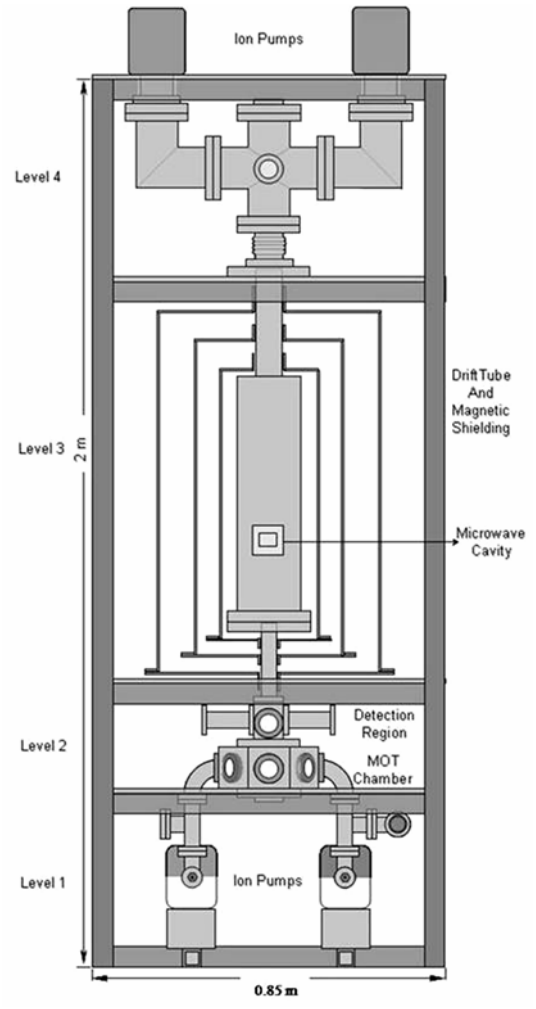

Figure 4. Schematics of physics package of the NPLI fountain.

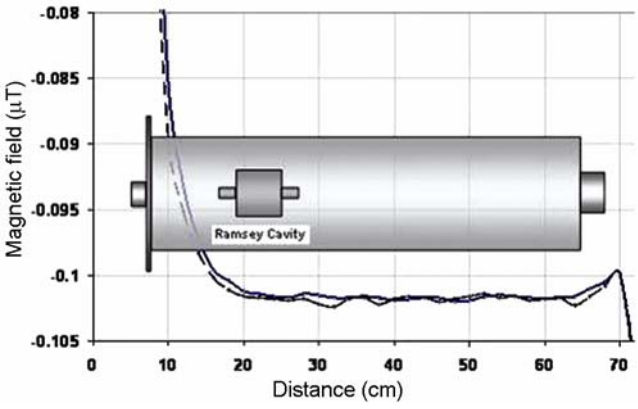

Figure 5. Experimental observations of the C-field variation in the drift region.

locked to a 5 MHz quartz oscillator via a divider chain (9600 : 8 : 3 : 4 : 20). Along the way, a signal of 407.37 MHz is generated with the help of direct digital synthesis (DDS). The required interrogation frequency is obtained by mixing (9600 MHz – 407.37 MHz = 9192.63 MHz). The signal from the atoms is then used to steer the 5 MHz quartz frequency.

The schematic of the fountain controller is shown in Figure 6. There are four autonomous microcontroller cards for timing sequence generation, AOM2 frequency sweep generation, launch frequency generation and amplitude ramp generation.

The fountain timing sequence generation, as shown in Figure 7, controls MOT current, RF frequency and power of the AOM drivers, mechanical shutters, photodiode gate and power to state selection cavity to run the process from MOT loading to polarization gradient cooling and measurement of time of flight signal. As shown in Figures 7, $t0$, $t1$, ..., $t10$ indicate times when a new action/cycle begins. Input parameters a, b, c, d, f, g, i and j are resettable independent variables and indicate time intervals for specific actions. For example, a is the MOT duration, b the OM duration after MOT, c the duration when horizontal lasers are off for launch, d the launch and post-cooling phase duration, g the blowout duration, i the detection window start delay, and j is the detection window duration. Typical values of a, b, c, d, g, i and j are 100, 50, 1, 4, 5, 10 and 10 ms respectively. The timing sequence generator microcontroller card receives information about the timings from the PC as serial inputs, as shown in Figure 6.

A detailed characterization of MOT has been done recently. The number of atoms in the trap was determined from the fluorescence signal. For calculating the number of atoms, fluorescence signal from the cold cloud was collected on a large-area silicon photodiode using imaging optics consisting of lenses and irises. As the size of this photodiode, its spectral response and distance to the trapped atoms is known, one could calculate the overall power of the emitted fluorescence light which enables one to measure the number of atoms[16].

The number of trapped atoms depends upon several MOT parameters such as intensity and diameter of the laser beams, magnetic field gradient, frequency detuning, etc. With appropriate operating parameters, we could cool and trap the cloud of cesium atoms with 10^7 atoms at the centre of MOT. In addition, dependence of total number of atoms on the magnetic field gradient and frequency detuning was checked to optimize the operating parameters. Figure 8 *a* shows how the number of atoms depends on magnetic field gradient at a fixed detuning. Figure 8 *b* shows how the number of atoms depends on detuning at a

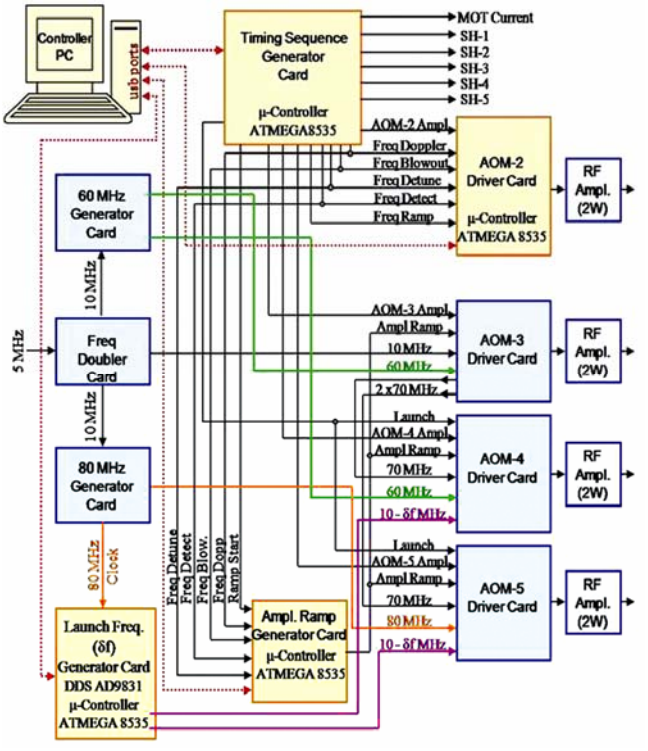

Figure 6. Schematic of the fountain controller for AOMs, shutters and magneto-optical trap current.

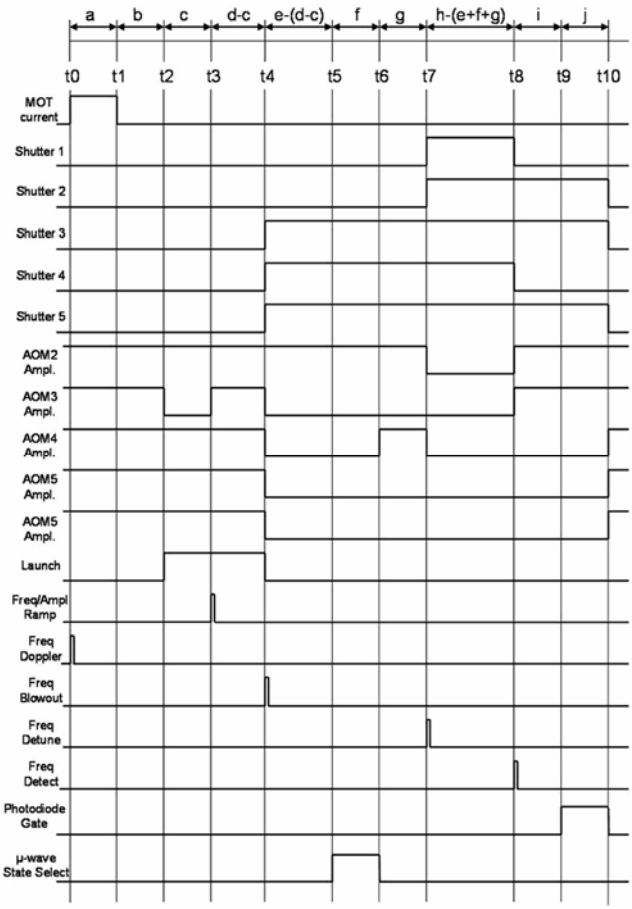

Figure 7. Graphical layout of the timing sequence.

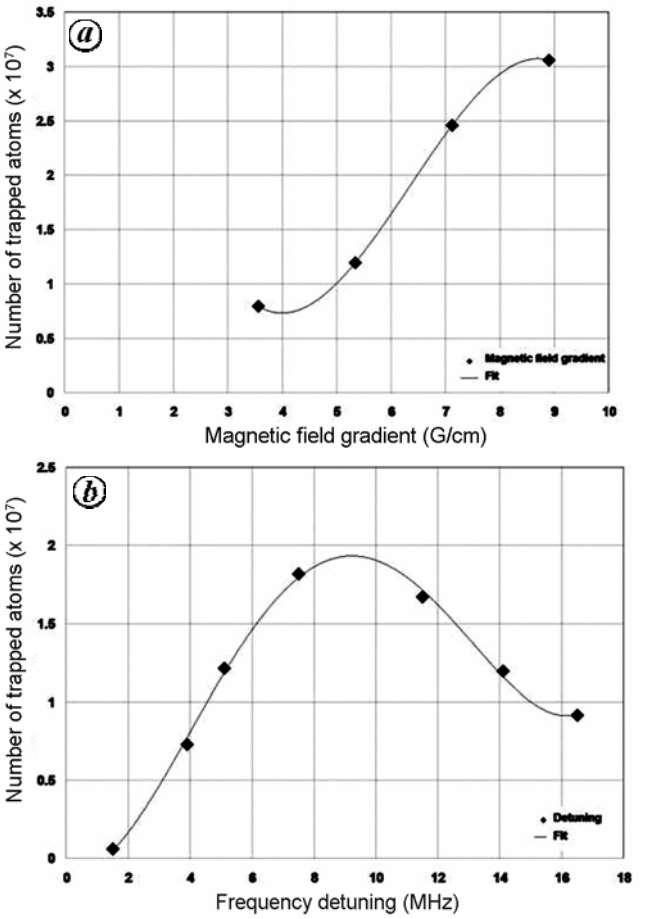

Figure 8. Number of trapped atoms as function of (***a***) magnetic field gradient, with 14.1 MHz detuning and (***b***) laser frequency detuning, with a magnetic field gradient of 5.34 G/cm.

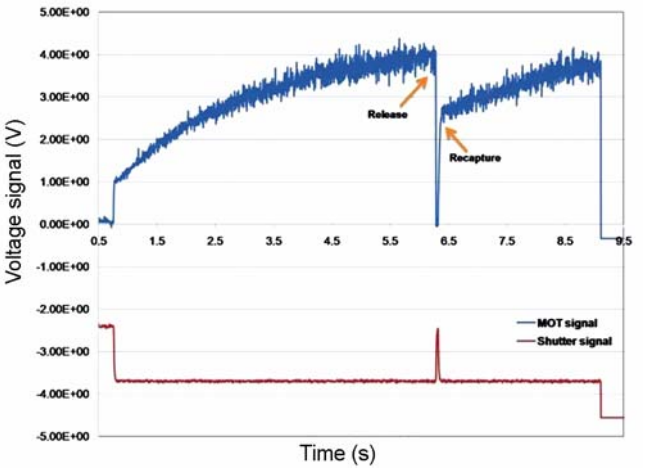

Figure 9. Fluorescence signal from the MOT and shutter signal as a function of time.

fixed magnetic field gradient. The results are in agreement with previously reported works[17,18].

The size of the cold atom cloud is determined from the CCD image. The pixel output value of CCD camera is proportional to the light intensity. The trapped atom cloud has a Gaussian density distribution. A two-dimensional picture of the MOT is taken using a CCD camera. Using the Matlab program, Gaussian function is fitted to the intensity values in both X and Y directions. To determine the size, CCD camera with lens system is calibrated by keeping a metric scale in a similar configuration. Assuming spherical symmetry, the typical Gaussian half-width diameter of the cloud is estimated. In our case, the cloud size (diameter) was estimated to be 1.5 mm for a magnetic field gradient of 2.1 G/cm and detuning of 14.1 MHz.

The temperature of the cloud was measured using release and recapture method. Release and recapture method is one of the simplest techniques first used by Chu and his collaborators in their study of Doppler cooling of atoms in OM[19]. A similar technique is used here to measure the temperature of cold atoms trapped in a MOT. MOT beams are turned off for time t. The fluorescence signal from the cloud is recorded using a photodetector, as explained earlier. In the absence of MOT beams and trapping field, atoms are expanded ballistically and go out of the detection region, which is imaged by a lens on the photo detector. The fraction of remaining atoms in the detection region is detected in the fluorescence signal by turning on MOT beams. Using the fraction of atoms captured on turning back MOT beams after light-off time Δt and initial size of the cloud, temperature of the cloud is calculated[16].

Figure 9 shows the release and recapture signal observed using an oscilloscope. After MOT reaches saturation, all six confining beams are switched off with the help of shutters for 25 ms. During this time, atoms leave the trap centre with their instantaneous velocities. When the beams are turned back again, a fraction of the atoms is captured at the trap centre as shown in Figure 9. From these data, the temperature of the cloud is calculated for different light-off times, and the average temperature of the cloud in the MOT was about 125 μK.

A detailed description of the progress in building NPLI Cs fountain has been presented here. The present status of progress is (i) the entire optics is assembled and operational, (ii) the mechanical assembly of the fountain is complete, (iii) the necessary level of vacuum for cooling and launching of atoms has been attained, (iv) most of the electronics has been designed and tested, and (v) characterization of cold atoms in the MOT has been done.

We are now ready to perform initial experiments with launching the atom cloud and performing Ramsey interrogation. The evaluation and characterization of the complete, first ever primary frequency standard of time and frequency in India will be done subsequently.

1. Wynands, R. and Weyers, S., Atomic fountain clocks. *Metrologia*, 2005, **42**, 64–79.
2. Meekhof, D. M., Jefferts, S. R., Stepanovic, M. and Parker, T. E., Accuracy evaluation of a cesium fountain frequency standard at NIST. *IEEE Trans. Instrum. Meas.*, 2001, **50**, 507–509.

3. Weyers, S., Huebner, U., Schroeder, R., Tamm, C. and Bauch, A., Uncertainty evaluation of the atomic cesium fountain of the PTB. *Metrologia*, 2001, **38**, 343–352.
4. Marmet, L., Hoger, B., Dubé, P., Madej, A. A. and Bernard, J. E., Detailed description of FCs1: NRC's cesium fountain primary standard. In Proceedings of the 2008 IEEE International Frequency Control Symposium, 2008, p. 386.
5. Szymaniec, K., Chalupczak, W. and Henderson, D., Initial evaluation of the NPL caesium fountain frequency standard. In Proceedings of the 2003 IEEE International Frequency Control Symposium and PDA Exhibition, 2003, p. 112.
6. Kumagai, M., Ito, H., Fukuda, K., Kajita, M., Hosokawa, M. and Morikawa, T., Development of Cs atomic fountain frequency standard at CRL. In Proceedings of the 2003 IEEE International Frequency Control Symposium and PDA Exhibition, 2003, p. 120.
7. Kumagai, M., Ito, H., Kajita, M. and Hosokawa, M., Recent results of NICT caesium atomic fountains. In Proceedings of European Frequency and Time Forum 07 (EFTF07), Geneva, Switzerland, 2007, pp. 602–606.
8. Kwon, T. Y., Lee, H. S., Yang, S. H. and Park, S. E., Development of a cesium atomic fountain frequency standard. *IEEE Trans. Instrum. Meas.*, 2003, **52**, 263–266.
9. Levi, F., Lorini, L., Calonico, D., Bertacco, E. K. and Godone, A., IEN-CsF1 accuracy evaluation and two way frequency comparison. In Proceedings of the 2003 IEEE International Frequency Control Symposium and PDA Exhibition, 2003, p. 199.
10. Clairon, A., Laurent, Ph., Santarelli, G., Ghezali, S., Lea, S. N. and Bahoura, M., A cesium fountain frequency standard: preliminary results. *IEEE Trans. Instrurm. Meas*., 1995, **IM44**, 128–131.
11. Sen Gupta, A., Agarwal, A., Arora, P. and Pant, K., Progress in building of cesium fountain frequency standard at NPL, India. In CPEM 2010 Technical Digest, 2010.
12. Weyers, S., Hübner, U., Schröder, R., Tamm, Chr. and Bauch, A., Uncertainty evaluation of the atomic caesium fountain CSF1 of the PTB. *Metrologia*, 2001, **38**, 343–352.
13. Donley, E. A., Heavner, T. P., Levi, F., Tataw, M. O. and Jefferts, S. R., Double-pass acousto-optic modulator system. *Rev. Sci. Instrum.*, 2005, **76**, 063112.
14. Schröder, R., Hübner, U. and Griebsch, D., Design and realization of the microwave cavity in the PTB caesium atomic fountain clock CsF1. *IEEE Trans. Ultrasonics, Ferroelectri. and Frequency Control*, 2002, **49**, 383–392.
15. Sen Gupta, A., Schröder, R., Weyers, S. and Wynands, R., A new 9 GHz synthesis chain for atomic fountain clocks. In Proceedings of the European Frequency and Time Forum 07 (EFTF07), Geneva, Switzerland, 2007, pp. 234–237.
16. Mahopatra, A. K., Study of atom–surface interactions using laser-cooled atoms. Ph D thesis, TIFR Mumbai, 2005.
17. Lopez, M., Carlos, E., Talavera, M. and Lopez, S., Progress at CENAM towards a Cs Fountain Clock. In Proceedings of Multiconference on Electronics and Photonics 06 (MEP 06), Guanjuato, Mexico, 2006, p. 114.
18. Lindquist, K., Stephens, M. and Wieman, C., Experimental and theoretical study of the vapor-cell Zeeman optical trap. *Phys. Rev. A*, 1992, **46**, 4082–4090.
19. Chu, S., Hollberg, L., Bjorkholm, J. E., Cable, A. and Ashkin, A., Three dimensional viscous confinement and cooling of atoms by resonance radiation pressure. *Phys. Rev. Lett.*, 1985, **55**, 48–51.

ACKNOWLEDGEMENTS. We thank the present and former Directors of NIPL, New Delhi – Drs R. C. Budhani, V. Kumar, K. Lal and A. K. Raychoudhury for sustained support and encouragement to the NPLI fountain project. We acknowledge technical help and cooperation from colleagues of the Time & Frequency Division of PTB, Germany and NIST, Boulder, USA.

Received 1 September 2010; revised accepted 28 February 2011

An assay for screening anti-mitotic activity of herbal extracts

G. Satyanarayana Murthy[1,*], T. P. Francis[1], C. Rajendra Singh[2], H. G. Nagendra[2] and Chandrashekhar Naik[2]

[1]Herbal Science Trust, #100 Residency Road, Bangalore 560 025, India
[2]Department of Biotechnology, Sir M. Visvesvaraya Institute of Technology, Bangalore 562 157, India

The Herbal Science Trust (HST), Bangalore has developed an effective palliative herbal extract (HST-K) for the management of pain in terminal cancer patients. We were interested in the purification of the anti-mitotic/therapeutic (referred as bioactivity) component in HST-K. In pursuit of this goal we have developed an *in vitro* method for quantification of the bioactivity in HST-K, based upon the observation that the sprouting of green-gram seed was inhibited by HST-K. The inhibition was found to be dose-dependent and was suitable to quantify the bioactivity of HST-K preparations. The method was further extended as an easy screening procedure for anti-mitotic activity of herbal extracts. Synthetic drugs useful for palliation in cancer also inhibited the sprouting of green-gram seeds, whereas other common drugs failed to inhibit sprouting. We have identified a few common vegetables, viz. onion, garlic and capsicum as anti-mitotic using the above screening method.

Keywords: Anti-mitotic activity, herbal extracts, germination, sprouting, inhibition.

THE gift of health to humanity by scientific methods in the war-ravaged European continent in the last 300 years has been unconditionally recognized all over the world today. Despite such achievements, we have not been able to understand the etiology of cancer, and scientific methods can only provide poor palliation. Treatments like chemotherapy, radiotherapy and surgery provide only partial and transient relief. In the 1950s–70s, attempts were made in the West to develop alternate systems for cancer management[1], but these have been inconclusive[2]. Recently, the National Institutes of Health, USA has approved trials of alternate systems of medicine for cancer under 'investigative new drug' development scheme. Under this scheme, treatment by unorthodox medication from alternate systems is legally permitted to be tried on willing patients.

India, the home of Ayurveda, has many references to the management of tumours in texts like *Astanga Hrudaya*[3]. These references are indirect and have to be identified by a careful study of the texts. The Herbal Science Trust (HST), Bangalore is involved in identifying such

*For correspondence. (e-mail: gundlupet_murthy@yahoo.co.in)